Less Symmetrical Dicopper(II) Complexes as Catechol Oxidase Models—An Adjacent Thioether Group Increases Catecholase Activity

Michael Merkel,[a] Niclas Möller,[a] Manuel Piacenza,[b] Stefan Grimme,*[b] Annette Rompel,[a] and Bernt Krebs*[a]

Dedicated to Professor Arndt Simon on the occasion of his 65th birthday

Abstract: Three new unsymmetrical compartmental dinucleating ligands, 4-bromo-2-(4-methylpiperazin-1-ylmethyl)-6-[{2-(1-piperidyl)ethyl}aminomethyl]phenol (HL1), 4-bromo-2-(4-methylpiperazin-1-ylmethyl)-6-[{2-(morpholin-4-yl)ethyl}aminomethyl]phenol (HL2), and 4-bromo-2-(4-methylpiperazin-1-ylmethyl)-6-[{2-(thiomorpholin-4-yl)ethyl}aminomethyl]phenol (HL3), have been synthesized in order to model the active site of type 3 copper proteins. The dicopper(II) complexes of these ligands give first hints about the influence of a thioether group close to the metal site. The bromophenol-based ligands have one piperazine arm and one other bidentate arm in positions 2 and 6 of the phenolic ring, respectively. With each ligand a dinuclear copper(II) complex was prepared and structurally characterized. The copper ions were found to have square pyramidal environments and a mixture of endogenous phenoxo and exogenous acetate bridging. The influence of a heteroatom in one arm of the ligand on catecholase activity and speciation in solution was studied by UV/Vis spectroscopy, ESI-MS experiments and, DFT calculations.

Keywords: bioinorganic chemistry · catechol oxidase · copper · enzyme models · structure–property relationships

Introduction

Transport, activation, and metabolism of dioxygen are very important processes in many living organisms. Metalloproteins containing one or more copper centers are often responsible for these functions.[1] The so-called type 3 copper proteins have an antiferromagnetically coupled dicopper core with three histidine ligands on each copper ion and μ-hydroxo bridging in the *met*-Cu^{II}–Cu^{II} form, which results in an EPR-silent active site. Well-known representatives of type 3 copper proteins are hemocyanin, the dioxygen carrier and transport protein for arthropods and molluscs,[2,3] tyrosinase, which catalyzes the hydroxylation of phenols to catechols (cresolase activity) and the oxidation of catechols to quinones (catecholase activity),[4] and catechol oxidase (CO) that exhibits only catecholase activity. CO was first isolated by Kubowitz in 1937 from potatoes.[5,6] Since then COs have been purified from different sources, among which are potatoes, spinach, apples, grape berries,[7] lychee fruit,[8] beans,[9] bananas,[10] opium plants,[11] coffee plants,[12] black poplars,[13] and gypsy wort.[13]

A new insight into the catalytic mechanism of catechol oxidases was gained with the determination of the crystal structure of the enzyme from sweet potatoes (*Ipomoea batatas*; ibCO).[14] Even though the first coordination sphere of each copper center consists of three histidines and one μ-OH bridge, both copper ions were found to be nonequivalent. The most striking asymmetric feature is a covalent thioether bond formed between the C_ε atoms of His109 and Cys92. A cysteinyl–histidinyl bond has also been reported for other type 3 copper proteins, like tyrosinase from *Neurospora crassa*[15] and hemocyanin from *Helix pomatia*[16] and *Octopus dofleini*.[17] A thioether bond between cysteine and tyrosine is also present in the mononuclear copper enzyme galactose oxidase.[18] Biomimetic models mimicking this feature were presented by Wieghardt and co-workers.[19]

A wide range of work has been done in the field of biomimetic model compounds for type 3 copper proteins. It has

[a] Dr. M. Merkel, Dr. N. Möller, Dr. A. Rompel, Prof. Dr. B. Krebs
Institut für Anorganische und Analytische Chemie der Westfälischen Wilhelms-Universität
Wilhelm-Klemm-Strasse 8, 48149 Münster (Germany)
Fax: (+49) 251-8338-366
E-mail: krebs@uni-muenster.de

[b] Dr. M. Piacenza, Prof. Dr. S. Grimme
Organisch-Chemisches Institut der Westfälischen Wilhelms-Universität
Corrensstrasse 40, 48149 Münster (Germany)
Fax: (+49) 251-8336-515
E-mail: grimmes@uni-muenster.de

Supporting information for this article is available on the WWW under http://www.chemeurj.org/ or from the author.

 DOI: 10.1002/chem.200400768 © 2005 Wiley-VCH Verlag GmbH & Co. KGaA, Weinheim

been summarized in a number of articles.[20–33] Model compounds that seize the idea of asymmetry might especially help to elucidate important questions concerning the binding of the substrate in the natural enzyme: for example, does the catecholate bridge the two copper(II) centers[1,34] or is it only bound to one metal center?[35] Dinuclear copper complexes employing the model substrate tetrachlorocatecholate have proven that both binding modes can be realized.[36,37]

Some dinuclear copper compounds from compartmental ligands have already been reported.[38–44] In this work, we have prepared three new dinucleating N_4O donor ligands (Scheme 1) to mimic the unsymmetric active site in catechol oxidase, 4-bromo-2-(4-methylpiperazin-1-ylmethyl)-6-[{2-(1-piperidyl)ethyl}aminomethyl]phenol (HL1), 4-bromo-2-(4-methylpiperazin-1-ylmethyl)-6-[{2-(morpholin-4-yl)ethyl}-aminomethyl]phenol (HL2), and 4-bromo-2-(4-methylpiperazin-1-ylmethyl)-6-[{2-(thiomorpholin-4-yl)ethyl}aminomethyl]phenol (HL3). These compartmental ligands build different coordination surroundings for two copper ions in close proximity. This proximity is important, since EXAFS data suggest a Cu–Cu distance of 2.9 Å for the *met*-form of the enzyme.[45] Furthermore, one arm of the ligand is modified from piperidine (L1) to morpholine (L2) and finally thiomorpholine (L3). The effects of these variations, including the introduction of the thioether group in HL3, on catecholase activity and speciation in solution were studied. For the adjacent thioether group, we observed an involvement in metal coordination. Thus, its function in these metal compounds is different from that in type 3 copper proteins, where metal coordination of the thioether group is not likely.

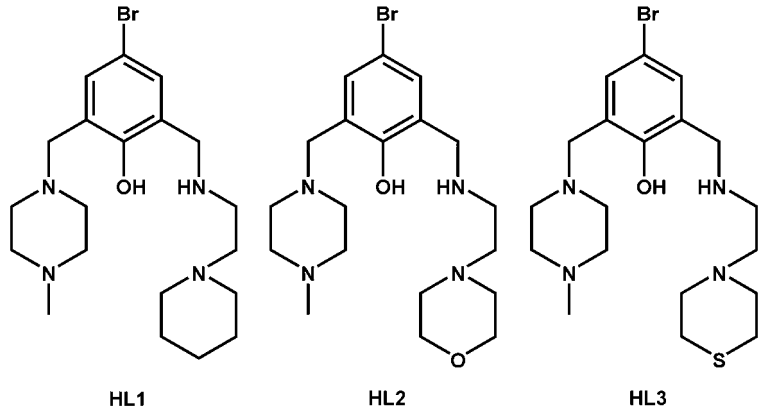

Scheme 1. Structures of the compartmental phenol-based ligands HL1–HL3.

Experimental Section

Materials: All chemicals were purchased from commercial sources and used without any further purification.

Physical measurements: ^{1}H and ^{13}C NMR spectra were recorded on a Bruker WH 300 instrument; all chemical shifts are reported relative to an internal standard of tetramethylsilane. Elemental analyses were performed on a Heraeus CHN-O-RAPID or an ELEMENTAR Vario El III analyzer. Electronic spectroscopy was carried out with a Hewlett–Packard 8453 diode array spectrometer by using quartz cuvettes (1 cm, methanolic solutions, 5×10^{-4} M). IR spectra (in KBr or Nujol) were recorded on a Bruker IF 48 Fourier transform spectrometer; FIR spectra (in polyethylene) were recorded on a Bruker IF 113v instrument. ESI-MS measurements were performed on a Micromass Quattro LC instrument.

Ligands: The to-date-unknown compartmental ligands 4-bromo-2-(4-methylpiperazin-1-ylmethyl)-6-[{2-(1-piperidyl)ethyl}aminomethyl]phenol (HL1), 4-bromo-2-(4-methylpiperazin-1-ylmethyl)-6-[{2-(morpholin-4-yl)ethyl}aminomethyl]phenol (HL2), and 4-bromo-2-(4-methylpiperazin-1-ylmethyl)-6-[{2-(thiomorpholin-4-yl)ethyl}aminomethyl]phenol (HL3) were synthesized according to a route described by Fenton and co-workers.[46] The first step in the synthesis of all three ligands is a Mannich reaction of 5-bromo-2-hydroxybenzaldehyde with *N*-methylpiperazine and paraformaldehyde to produce 4-bromo-2-formyl-6-(4-methylpiperazin-1-ylmethyl)phenol.[47] *N*-(2-aminoethyl)piperidine and *N*-(2-aminoethyl)morpholine were obtained from commercial sources, whereas *N*-(2-aminoethyl)thiomorpholine was synthesized following a literature procedure.[48]

General procedure: 4-Bromo-2-formyl-6-(4-methylpiperazin-1-ylmethyl)phenol (3.74 g, 12 mmol) was dissolved in ethanol (40 mL). One equivalent of the corresponding amine (1.54 g of *N*-(2-aminoethyl)piperidine for HL1, 1.56 g of *N*-(2-aminoethyl)-morpholine for HL2, and 1.76 g of *N*-(2-aminoethyl)thiomorpholine for HL3, respectively) was added and the reaction mixture was heated to reflux for 3 h. At 0 °C, sodium borohydride (1.21 g, 36 mmol) was carefully added. The resulting suspension was stirred overnight at room temperature and once again heated to reflux for 1 h. To destroy excess borohydride, hydrochloric acid was added to the reaction mixture, which was then stirred vigorously for 30 minutes. Afterwards, the pH value was adjusted to 8 by addition of sodium hydroxide solution and the resulting precipitate was removed by filtration. The filtrate was concentrated under reduced pressure and the residue was taken up in chloroform and dried over sodium sulfate. Filtration and removal of the solvent yielded the product as a yellowish, highly viscous oil.

HL1: Yield: 3.82 g (7.67 mmol, 64 %); ^{1}H NMR (300 MHz, $CDCl_3$): $\delta=$ 1.49 (m, 4H; CH_2), 1.66 (m, 2H; CH_2), 2.25 (s, 3H; CH_3), 2.55 (t, 4H; CH_2), 2.56 (br s, 4H; CH_2), 2.63 (br s, 4H; CH_2), 2.74 (t, 2H; CH_2), 2.95 (t, 2H; CH_2), 3.68 (s, 2H; CH_2), 3.96 (s, 2H; CH_2), 7.12 (s, 1H; CH_{ar}), 7.29 (s, 1H; CH_{ar}), 8.09 (br s, 1H, OH) ppm; ^{13}C NMR (75 MHz, $CDCl_3$): $\delta=$23.8 (CH_2), 25.3 (CH_2), 44.0 (CH_2), 45.8 (CH_3), 48.1 (CH_2), 52.5 (CH_2), 54.2 (CH_2), 54.8 (CH_2), 55.6 (CH_2), 56.7 (CH_2), 110.9 (C_{ar}), 123.3 (C_{ar}), 124.0 (C_{ar}), 131.5 (C_{ar}), 132.0 (C_{ar}), 155.7 (C_{ar}) ppm; IR (Nujol): $\tilde{\nu}=$ 3498 (s), 2939 (m), 2849 (m), 2798 (m), 2448 (w), 1608 (m), 1457 (s), 1398 (w), 1367 (m), 1350 (m), 1299 (m), 1284 (m), 1233 (m), 1160 (m), 1135 (m), 1092 (m), 1051 (m), 1008 (m), 986 (m), 920 (w), 867 (m), 819 (m), 781 (w), 754 (m), 728 (w), 660 (w), 624 (w), 559 (w), 542 (w), 491 (w), 442 (w) cm^{-1}; MS (ESI): *m*/*z*: 425–430 [M^+–H isotope cluster]; elemental analysis: calcd (%) for $C_{20}H_{33}BrN_4O$ (425.4): C 56.47, H 7.82, N 13.17; found: C 55.98, H 7.94, N 12.34.

HL2: Yield: 3.79 g (8.88 mmol, 74 %); ^{1}H NMR (300 MHz, $CDCl_3$): $\delta=$ 2.30 (s, 3H; CH_3), 2.38 (m, 4H; CH_2), 2.44 (t, 2H; CH_2), 2.54 (br s), 4H; CH_2), 2.59 (br s, 4H; CH_2), 2.66 (t, 2H; CH_2), 3.62 (m, 4H; CH_2), 3.68 (s, 2H; CH_2), 3.99 (s, 2H; CH_2), 7.12 (s, 1H; CH_{ar}), 7.29 (s, 1H; CH_{ar}) ppm;

© 2005 Wiley-VCH Verlag GmbH & Co. KGaA, Weinheim

^{13}C NMR (75 MHz, $CDCl_3$): δ = 43.8 (CH_3), 45.7 (CH_2), 48.0 (CH_2), 52.3 (CH_2), 53.2 (CH_2), 54.7 (CH_2), 55.5 (CH_2), 59.9 (CH_2), 66.9 (CH_2), 110.8 (C_{ar}), 123.1 (C_{ar}), 123.5 (C_{ar}), 131.5 (C_{ar}), 132.0 (C_{ar}), 155.6 (C_{ar}) ppm; IR (KBr): $\tilde{\nu}$ = 3439 (m), 2936 (m), 2797 (m), 2076 (w), 1887 (w), 1653 (w), 1606 (w), 1455 (s), 1390 (w), 1367 (w), 1348 (w), 1293 (w), 1226 (w), 1160 (m), 1136 (m), 1095 (m), 1010 (m), 920 (w), 868 (w), 815 (m), 748 (w), 623 (w), 489 (w), 441 (m) cm^{-1}; MS (ESI): *m*/*z*: 427–431 [M^+−H isotope cluster]; elemental analysis: calcd (%) for $C_{19}H_{31}BrN_4O_2$ (427.4): C 53.40, H 7.31, N 13.11; found: C 52.67, H 7.44, N 12.81.

HL3: Yield: 4.42 g (9.97 mmol, 83%); ^{1}H NMR (300 MHz, $CDCl_3$): δ = 2.30 (s, 3H; CH_3), 2.55 (m, CH_2), 2.60 (t, 2H; CH_2), 2.70 (m, CH_2), 2.90 (t, 2H; CH_2), 3.70 (s, 2H; CH_2), 3.90 (s, 2H; CH_2), 7.11 (s, 1H; CH_{ar}), 7.31 (s, 1H; CH_{ar}) ppm; ^{13}C NMR (75 MHz, $CDCl_3$): δ = 27.8 (CH_2), 44.0 (CH_3), 45.6 (CH_2), 48.0 (CH_2), 52.3 (CH_2), 54.6 (CH_2), 54.7 (CH_2), 55.5 (CH_2), 59.9 (CH_2), 110.8 (C_{ar}), 123.0 (C_{ar}), 131.6 (C_{ar}), 132.0 (C_{ar}), 155.6 (C_{ar}) ppm; IR (KBr): $\tilde{\nu}$ = 3393 (m), 2939 (m), 2807 (m), 1608 (w), 1459 (s), 1397 (w), 1365 (w), 1348 (w), 1285 (m), 1233 (m), 1160 (m), 1135 (m), 1087 (w), 1008 (w), 960 (w), 918 (w), 870 (w), 818 (m), 753 (s), 663 (w), 623 (w), 560 (w), 491 (w), 441 (w) cm^{-1}; MS (ESI): *m*/*z*: 443–447 [M^+−H isotope cluster]; elemental analysis: calcd (%) for $C_{19}H_{31}BrN_4OS$ (443.5): C 51.46, H 7.05, N 12.63; found: C 51.34, H 7.35, N 12.49.

Metal complexes

General procedure: A solution of copper(II) tetrafluoroborate hydrate (47 mg, 0.2 mmol in acetonitrile/methanol (1:1; 2 mL)) and a solution of copper(II) acetate hydrate (40 mg, 0.2 mmol in acetonitrile/methanol (1:1; 2 mL)) were added to a stirred solution of the ligand (0.2 mmol; HL1: 85 mg, HL2: 86 mg, or HL3: 89 mg, respectively) in acetonitrile/methanol (1:1; 2 mL), then triethylamine (eight drops) was added. The color of the solution changed from green to green-blue. After being stirred for 10 min, the reaction mixture was filtered and vapor diffusion of diethyl ether into the complex solution afforded dark green cuboid shaped crystals of $[Cu_2(L1)(\mu\text{-}OAc)_2](BF_4)$ (**1**), $[Cu_2(L2)(\mu\text{-}OAc)_2](BF_4)$ (**2**), or $[Cu_2(L3)(\mu\text{-}OAc)_2](BF_4)$ (**3**), respectively.

$[Cu_2(L1)(\mu\text{-}OAc)_2](BF_4)\cdot 0.25\,Et_2O$ (1): Yield: 68 mg (0.09 mmol, 47%); m.p. 240°C (decomp); IR (KBr): $\tilde{\nu}$ = 3420 (m), 3256 (m), 2931 (m), 2868 (m), 1607 (s), 1462 (m), 1446 (m), 1415 (s), 1361 (w), 1340 (w), 1297 (w), 1276 (w), 1242 (m), 1182 (w), 1082 (s), 950 (w), 931 (w), 893 (w), 876 (w), 810 (m), 773 (m), 757 (m), 662 (m), 645 (w), 630 (w), 615 (w), 586 (w), 561 (w), 522 (w), 464 (w) cm^{-1}; FIR: $\tilde{\nu}$ = 371 (w), 350 (m), 284 (s), 259 (m), 231 (m), 208 (s), 164 (m), 133 (w), 85 (m) cm^{-1}; elemental analysis: calcd (%) for $C_{24}H_{38}Cu_2BBrF_4N_4O_5$ (756.4; without solvent): C 38.11, H 5.06, N 7.41; found: C 37.82, H 5.11, N 7.45.

$[Cu_2(L2)(\mu\text{-}OAc)_2](BF_4)$ (2): Yield: 83 mg (0.11 mmol, 53%); m.p. 205°C (decomp); IR (KBr): $\tilde{\nu}$ = 3435 (m), 3275 (m), 3069 (w), 2971 (m), 2930 (m), 2901 (m), 2869 (m), 2817 (w), 1603 (s), 1420 (s), 1394 (s), 1358 (w), 1338 (w), 1306 (w), 1279 (m), 1241 (m), 1180 (w), 1057 (s), 988 (s), 953 (m), 928 (m), 904 (w), 887 (m), 842 (m), 809 (m), 770 (m), 659 (m), 634 (m), 612 (w), 595 (w), 576 (w), 519 (w), 465 (w) cm^{-1}; FIR: $\tilde{\nu}$ = 395 (w), 368 (w), 350 (s), 271 (w), 245 (m), 203 (m), 178 (s), 150 (m) cm^{-1}; elemental analysis: calcd (%) for $C_{23}H_{36}Cu_2BBrF_4N_4O_6$ (758.4): C 36.43, H 4.78, N 7.38; found: C 36.36, H 4.69, N 7.43.

$[Cu_2(L3)(\mu\text{-}OAc)_2](BF_4)\cdot 0.25\,MeOH\cdot 0.75\,H_2O$ (3): Yield: 77 mg (0.10 mmol, 51%); m.p. 235°C (decomp); IR (KBr): $\tilde{\nu}$ = 3639 (w), 3562 (w), 3423 (w), 3262 (m), 2972 (m), 2923 (m), 2872 (m), 1614 (s), 1463 (s), 1414 (s), 1361 (w), 1338 (m), 1299 (m), 1279 (m), 1240 (m), 1181 (w), 989 (m), 964 (m), 883 (m), 866 (m), 810 (m), 774 (m), 756 (m), 662 (m), 644 (m), 629 (m), 589 (m), 559 (w), 522 (m), 458 (m) cm^{-1}; FIR: $\tilde{\nu}$ = 398 (m), 348 (m), 311 (m), 289 (w), 260 (m), 206 (m), 162 (m), 104 (w) cm^{-1}; elemental analysis: calcd (%) for $C_{23}H_{36}Cu_2BBrF_4N_4O_5S$ (774.4; without solvent): C 35.67, H 4.68, N 7.23; found: C 35.54, H 4.61, N 7.31.

X-ray crystal structures: The intensity data of compounds **1** and **3** were collected on an STOE IPDS diffractometer ($Mo_{K\alpha}$, λ = 0.71073 Å, graphite monochromator) by using the ϕ-scan technique. Data collection for compound **2** was performed on a Bruker AXS SMART APEX CCD diffractometer ($Mo_{K\alpha}$, λ = 0.71073 Å, graphite monochromator) by using the ω-scan technique. All structures were solved by direct methods and refined by full-matrix least-squares methods on F^2.[49] Further data collection parameters are summarized in Table 1. Selected bond lengths and angles for the dinuclear copper(II) complexes are reported in Table 2. The disordered solvent molecules in **1** and **3** were refined with isotropic displacement parameters and without hydrogen atoms, whereas all other

Table 1. Crystallographic data and experimental details.

	1	**2**	**3**
empirical formula	$C_{25}H_{40.5}BBrCu_2F_4N_4O_{5.25}$	$C_{23}H_{36}BBrCu_2F_4N_4O_6$	$C_{23.25}H_{38.5}BBrCu_2F_4N_4O_6S$
M_r	774.91	758.36	795.94
temperature [K]	213(2)	153(2)	213(2)
radiation, λ [Å]	$Mo_{K\alpha}$, 0.71073	$Mo_{K\alpha}$, 0.71073	$Mo_{K\alpha}$, 0.71073
crystal shape	green cuboid	green cuboid	green cuboid
crystal size [mm]	0.32×0.24×0.12	0.28×0.25×0.13	0.36×0.24×0.24
crystal system	triclinic	triclinic	triclinic
space group	$P\bar{1}$ (no. 2)	$P\bar{1}$ (no. 2)	$P\bar{1}$ (no. 2)
a [Å]	14.282(3)	10.410(5)	12.930(3)
b [Å]	16.612(3)	10.594(5)	16.088(3)
c [Å]	16.914(3)	14.245(5)	17.367(3)
α [°]	62.43(3)	78.330(5)	87.52(3)
β [°]	81.36(3)	69.750(5)	74.82(3)
γ [°]	68.14(3)	75.050(5)	78.34(3)
V [Å^3]	3300(2)	1413(2)	3415(2)
Z	4	2	4
ρ_{calcd} [g cm^{-3}]	1.522	1.783	1.548
μ [mm^{-1}]	2.562	2.991	2.534
F(000)	1578	768	1616
scan range 2θ [°]	8.66–52.20	3.08–56.54	8.78–52.06
index ranges	$-17 \le h \le 16$	$-13 \le h \le 13$	$-15 \le h \le 15$
	$-20 \le k \le 20$	$-13 \le k \le 14$	$-19 \le k \le 19$
	$-20 \le l \le 20$	$-18 \le l \le 18$	$-21 \le l \le 21$
reflections collected	26123	14766	27120
unique reflections	12088	6957	12442
reflections $I > 2\sigma(I)$	5739	5660	7159
R_{int}	0.1290	0.0247	0.0974
data/restraints/parameters	10902/0/739	6957/0/370	12439/0/740
goodness-of-fit on F^2	1.016	0.966	0.952
final *R* indices ($I > 2\sigma(I)$)			
*R*1	0.0717	0.0391	0.0857
*wR*2	0.1495[a]	0.1019[b]	0.2132[c]
R indices (all data)			
*R*1	0.1689	0.0488	0.1449
*wR*2	0.1880[a]	0.1057[b]	0.2401[c]
largest diff. peak/hole [e Å^{-3}]	0.697/−0.639	1.169/−0.627	1.081/−1.008

[a] $w = 1/[\sigma^2(F_o^2)+(0.0698P)^2+0.0090P]$ with $P = (F_o^2+2F_o^2)/3$. [b] $w = 1/[\sigma^2(F_o^2)+(0.0607P)^2]$ with $P = (F_o^2+2F_o^2)/3$. [c] $w = 1/[\sigma^2(F_o^2)+(0.0751P)^2+20.5428P]$ with $P = (F_o^2+2F_o^2)/3$.

 © 2005 Wiley-VCH Verlag GmbH & Co. KGaA, Weinheim

Table 2. Selected lengths [Å] and angles [°] in complexes **1–3**.

1					
Cu(1)···Cu(2)	3.304(2)	O(1)–Cu(1)–O(2)	97.7(3)	O(1)-Cu(2)-O(3)	92.2(2)
Cu(1)–O(1)	1.950(6)	O(1)-Cu(1)-O(4)	95.7(3)	O(1)-Cu(2)-O(5)	95.1(2)
Cu(1)–O(2)	1.965(6)	O(1)-Cu(1)-N(1)	91.7(3)	O(1)-Cu(2)-N(3)	91.4(3)
Cu(1)–O(4)	2.137(7)	O(1)-Cu(1)-N(2)	164.1(3)	O(1)-Cu(2)-N(4)	170.0(3)
Cu(1)–N(1)	2.042(7)	O(2)-Cu(1)-O(4)	99.7(3)	O(3)-Cu(2)-O(5)	96.9(3)
Cu(1)–N(2)	2.025(8)	O(2)-Cu(1)-N(1)	149.7(3)	O(3)-Cu(2)-N(3)	94.4(3)
Cu(2)–O(1)	1.965(5)	O(2)-Cu(1)-N(2)	94.3(3)	O(3)-Cu(2)-N(4)	96.8(3)
Cu(2)–O(3)	2.232(7)	O(4)-Cu(1)-N(1)	107.9(3)	O(5)-Cu(2)-N(3)	166.7(3)
Cu(2)–O(5)	1.937(6)	O(4)-Cu(1)-N(2)	92.4(3)	O(5)-Cu(2)-N(4)	88.3(3)
Cu(2)–N(3)	1.994(7)	N(1)-Cu(1)-N(2)	72.8(3)	N(3)-Cu(2)-N(4)	83.5(3)
Cu(2)–N(4)	2.107(7)			Cu(1)-O(1)-Cu(2)	115.1(3)
2					
Cu(1)···Cu(2)	3.263(2)	O(1)-Cu(1)–O(3)	91.5(1)	O(1)-Cu(2)-O(4)	96.1(1)
Cu(1)–O(1)	1.972(2)	O(1)-Cu(1)-O(5)	100.2(1)	O(1)-Cu(2)-O(6)	88.8(1)
Cu(1)–O(3)	2.163(2)	O(1)-Cu(1)-N(1)	92.4(1)	O(1)-Cu(2)-N(3)	91.0(1)
Cu(1)–O(5)	1.938(2)	O(1)-Cu(1)-N(2)	162.8(1)	O(1)-Cu(2)-N(4)	175.2(1)
Cu(1)–N(1)	2.018(2)	O(3)-Cu(1)-O(5)	107.9(1)	O(4)-Cu(2)-O(6)	102.9(1)
Cu(1)–N(2)	2.076(3)	O(3)-Cu(1)-N(1)	94.9(1)	O(4)-Cu(2)-N(3)	155.5(1)
Cu(2)–O(1)	1.954(2)	O(3)-Cu(1)-N(2)	98.4(1)	O(4)-Cu(2)-N(4)	88.1(1)
Cu(2)–O(4)	1.933(2)	O(5)-Cu(1)-N(1)	153.5(1)	O(6)-Cu(2)-N(3)	100.6(1)
Cu(2)–O(6)	2.278(2)	O(5)-Cu(1)-N(2)	90.2(1)	O(6)-Cu(2)-N(4)	88.0(1)
Cu(2)–N(3)	1.997(2)	N(1)-Cu(1)-N(2)	72.9(1)	N(3)-Cu(2)-N(4)	86.1(1)
Cu(2)–N(4)	2.063(2)			Cu(1)-O(1)-Cu(2)	112.4(1)
3					
Cu(1)···Cu(2)	3.299(2)	O(1)-Cu(1)-O(2)	99.4(3)	O(1)-Cu(2)-O(3)	91.2(3)
Cu(1)–O(1)	1.952(7)	O(1)-Cu(1)-O(4)	94.0(3)	O(1)-Cu(2)-O(5)	95.1(3)
Cu(1)–O(2)	1.935(8)	O(1)-Cu(1)-N(1)	91.5(3)	O(1)-Cu(2)-N(3)	90.9(3)
Cu(1)–O(4)	2.130(7)	O(1)-Cu(1)-N(2)	163.2(3)	O(1)-Cu(2)-N(4)	173.0(3)
Cu(1)–N(1)	2.028(9)	O(2)-Cu(1)-O(4)	104.7(3)	O(3)-Cu(2)-O(5)	100.2(3)
Cu(1)–N(2)	2.050(9)	O(2)-Cu(1)-N(1)	150.9(3)	O(3)-Cu(2)-N(3)	95.2(3)
Cu(2)–O(1)	1.974(6)	O(2)-Cu(1)-N(2)	91.4(4)	O(3)-Cu(2)-N(4)	94.4(3)
Cu(2)–O(3)	2.173(8)	O(4)-Cu(1)-N(1)	101.4(3)	O(5)-Cu(2)-N(3)	163.3(3)
Cu(2)–O(5)	1.917(7)	O(4)-Cu(1)-N(2)	95.7(3)	O(5)-Cu(2)-N(4)	87.8(3)
Cu(2)–N(3)	1.981(9)	N(1)-Cu(1)-N(2)	73.1(4)	N(3)-Cu(2)-N(4)	84.6(3)
Cu(2)–N(4)	2.128(8)			Cu(1)-O(1)-Cu(2)	114.3(3)

non-hydrogen atoms were refined anisotropically with ligand hydrogen atoms riding on ideal positions.[50]

Kinetic measurements: Catechol oxidase activities of complexes **1–3** were measured at 25 °C by time-dependent UV/Vis spectroscopy. 3,5-Di-*tert*-butylcatechol (5, 10, 20, 40, 50, 90, or 100 equivalents) dissolved in methanol was added to a sample (1 mL) of 2×10^{-4} M solutions of compounds **1–3** in methanol. The final sample volume was 2 mL and, accordingly, the concentration of the metal complex was 10^{-4} M. During the first 3 minutes of the reaction, the development of the absorption band at 400 nm was monitored. The average initial rates over three independent measurements were determined from the slope of the absorption versus time plot by utilizing the Lambert–Beer equation.

DFT calculations: All calculations were performed on a parallel LINUX-PC cluster by using the TURBOMOLE 5.3[51] program suite. All DFT calculations were carried out with the B3-LYP[52,53] density functional, and an *m3* numerical quadrature grid was applied in all DFT calculations. The resolution of identity (RI) approximation was used for the MP2[54] calculations. The basis sets were taken from the TURBOMOLE basis set library.[55] Basis sets of split-valence-double-ζ and split-valence-triple-ζ quality with polarization functions SV(d)[56] and TZV(d,p)[57] have been used. To simplify the calculations, the bromo substituent on the phenol spacer was treated as a hydrogen atom. The calculated energies refer to the corresponding complexes with two acetate bridges as the zero point.

Results and Discussion

Crystal structures of 1–3: All three compounds reported in this work crystallize in the centrosymmetric space group $P\bar{1}$. While the triclinic unit cell of **2** contains two formula units, the cells of **1** and **3** contain four formula units. The most likely reason for this is a reduction of the symmetry by the partly occupied solvent molecules in **1** and **3**. Since the two crystallographically independent complex cations in **1** and **3**, respectively, are chemically equivalent and show broad similarities, only one of them will be discussed for each compound. Ellipsoid plots of the cations in **1–3** are depicted in Figures 1–3, whereas selected bond lengths and angles are listed in Table 2.

The two copper ions in all three dinuclear $[Cu^{II}(L)(\mu\text{-}OAc)_2]^+$ complexes are μ-phenoxo-bridged by a deprotonated ligand. Furthermore, two exogenous acetate bridges are found in each complex. This bridging motif leads to Cu(1)–Cu(2) distances of 3.304(2) (**1**), 3.263(2) (**2**), and 3.299(2) Å (**3**). The remaining equatorial positions on each copper ion are occupied by nitrogen donors derived from the compartmental ligand, a fact result-

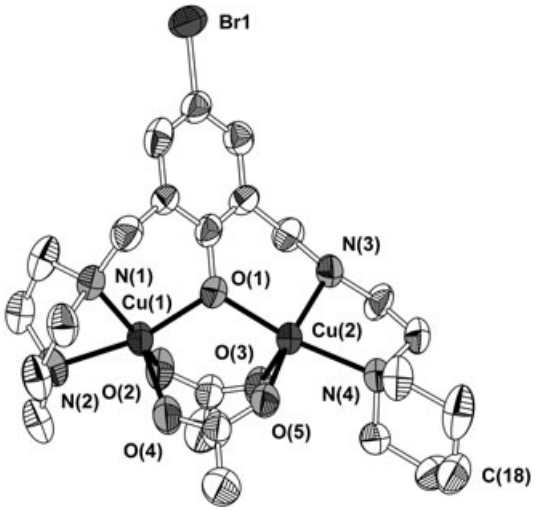

Figure 1. Representation of the cation in **1** (50% probability); the hydrogen atoms are omitted for clarity.

© 2005 Wiley-VCH Verlag GmbH & Co. KGaA, Weinheim

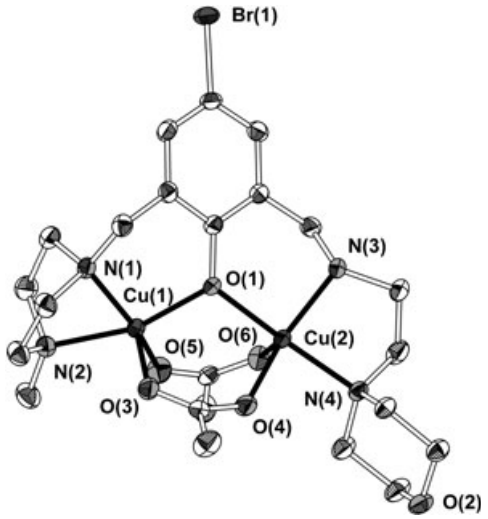

Figure 2. Representation of the cation in **2** (50% probability); the hydrogen atoms are omitted for clarity.

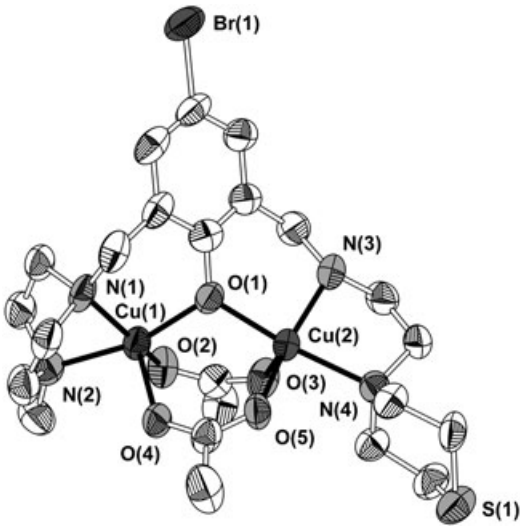

Figure 3. Representation of the cation in **3** (50% probability); the hydrogen atoms are omitted for clarity.

ing in a nonequivalent environment for the metal centers of each dinuclear unit. Cu(1) is, in all cases, coordinated by the two tertiary amines of the piperazine group (N(1) and N(2), respectively) that is found to be in its boat conformation, whereas Cu(2) is ligated by the secondary amine N(3) and the tertiary amine N(4) of the piperidine, morpholine or thiomorpholine group (in **1**–**3**, respectively). The piperazine nitrogen atoms are part of two five-membered chelate rings, while the nitrogen donors on Cu(2) are embedded in only one ring. The limited bite of these constellations leads to significantly narrowed angles between the corresponding donor atoms (N(1)-Cu(1)-N(2) = 72.8(3)/72.9(1)/73.1(4)° (**1**/**2**/**3**) and N(3)-Cu(2)-N(4) = 83.5(3)/86.1(1)/84.6(3)° (**1**/**2**/**3**)). The coordination polyhedra around the copper ions can be regarded as distorted square pyramidal with a shared corner. The τ values[58] are $\tau = 0.24$ and 0.06 for Cu(1) and Cu(2) in **1**, $\tau = 0.16$ and 0.33 for Cu(1) and Cu(2) in **2**, and $\tau = 0.21$ and 0.16 for Cu(1) and Cu(2) in **3**, respectively. Furthermore, the coordination polyhedra are stretched. This becomes evident in different apical and equatorial Cu–O bond lengths. The latter are about 0.2–0.3 Å larger in all cases. Calculations of the least-squares planes around Cu(1) and Cu(2) that contain the equatorial donor atoms reveal a displacement of the copper ions towards the apical ligands. In **1** Cu(1) is 0.305 Å and Cu(2) is 0.174 Å out of plane, whereas in **2** Cu(1) is 0.288 Å and Cu(2) is 0.173 Å out of plane, and in **3** Cu(1) is 0.309 Å and Cu(2) is 0.182 Å out of plane. All these deviations towards the apical donor lead to enlarged O_{apical}–Cu–X angles. The average values for these angles are 98.7 ° for Cu(1) and 95.2 ° for Cu(2). The phenolate oxygen atom is a shared edge of the two pyramids in all reported compounds with Cu(1)–O(1)–Cu(2) angles of 115.1(3) (**1**), 112.4(1) (**2**), and 114.3(3)° (**3**), respectively. The polyhedra are twisted against each other, which results in O_{apical}–Cu(1)–Cu(2)–O_{apical} torsion angles of 93.8(2) (**1**), 128.5(1) (**2**), and 102.8(4)° (**3**), respectively.

The intermolecular distances in compounds **1**–**3** suggest one (**1** and **2**) or two (**3**) hydrogen bonds between the tetrafluoroborate counter ions and the secondary amine N(3) atom with donor acceptor distances of 2.94(1)–3.23(1) Å.

Electronic spectra: In general, two kinds of transitions are expected for copper(II) complexes like **1**–**3**, d–d bands and ligand-to-metal charge transfer (LMCT) bands. In the presented compounds, the latter can either be phenolate–copper(II) or acetate–copper(II) transitions, which usually appear in the range from 300–340 nm.[59–62] However, in some cases these transitions were observed at wavelengths of up to 418 nm.[63] The phenolate-to-copper(II) charge transfer transition is particularly affected by the substituents on the phenolate and the electron density of the copper ions.[64] Finally, the intensity of these LMCT transitions is dependent

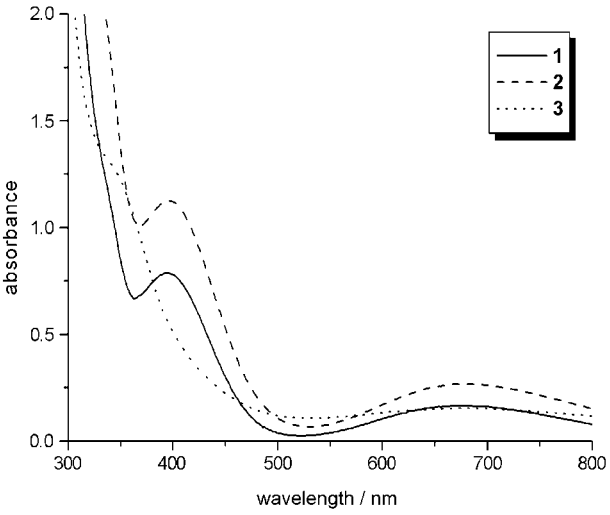

Figure 4. Electronic spectra of **1**–**3.**

 © 2005 Wiley-VCH Verlag GmbH & Co. KGaA, Weinheim

on the Cu–O–Cu angle, which correlates with the overlap of the phenolate p-orbital and the copper d-orbital.[61,65]

The electronic spectra of complexes **1–3** are depicted in Figure 4. Bands and extinction coefficients are summarized in Table 3. The absorption bands below 400 nm can be assigned to LMCT transitions, but it is not possible to distinguish between phenolate- and acetate-derived bands. Although the three compounds resemble each other, the spectrum of **3** differs from the others. The LMCT transition is shifted to higher energies and appears as a shoulder rather than as a distinct maximum. A possible explanation for this behavior would be an exchange of one or both acetate bridges by methanolates or hydroxides in solution. In the region of d–d transitions, all three complexes show a broad absorption with a maximum intensity at 675–680 nm that is indicative of their square-pyramidal geometries.[66,67]

Table 3. Summary of the UV/Vis spectroscopy data of **1–3**.

Compound	λ_{max} [nm]	ε [$M^{-1}cm^{-1}$]	λ_{max} [nm]	ε [$M^{-1}cm^{-1}$]
1	395	1575	675	331
2	397	2254	680	533
3	325-355 (sh)	-	677	307

Kinetic investigations: Air-saturated methanol solutions of **1–3** (10^{-4} M) were treated with 50 equivalents of 3,5-di-*tert*-butylcatechol. No base was added to the solutions in order to suppress oxidation of the substrate by base. The first apparent result, while the reaction was monitored by UV/Vis spectroscopy, was a significant activity, namely, a formation of a band at about 400 nm, which is indicative of an oxidation from 3,5-di-*tert*-butylcatchol to 3,5-di-*tert*-butyl-*o*-quinone. Consequently, the catecholase activity of all complexes was studied and saturation kinetics at high substrate concentrations were found for all compounds. Complex **3** was found to have the highest turnover number, with a rate of catalysis $k_{cat.} = 40.0 \pm 0.3\ h^{-1}$. The initial rates, as well as the Lineweaver–Burk plots are depicted in Figures S1–S6 in the Supporting Information. The results of the kinetic investigations are summarized in Table 4.

Table 4. Summary of the kinetic data of **1–3.**

Complex	$k_{cat.}$ [h^{-1}]	K_M[a] [$mol\,L^{-1}$]
1	10.7 ± 0.1	$(5.2 \pm 0.3) \times 10^{-3}$
2	28.9 ± 0.1	$(6.7 \pm 0.3) \times 10^{-4}$
3	40.0 ± 3	$(3.4 \pm 0.4) \times 10^{-3}$

[a] K_M = Michaelis constant.

The three model compounds presented in this work differ only in the nature of the heteroatom at position 4 of the ligand piperidine moiety. The different turnover numbers for the oxidation of 3,5-di-*tert*-butylcatechol give a first hint at the function of sulfur in these systems. In catalytic systems it is important to have free or labile coordination sites for substrate binding. In the solid states of compounds **1–3**, exogenous acetate bridges occupy these sites. Thus, research must be aimed at developing strategies to dissociate these bridges. A higher affinity of the heteroatom in the piperidine ring seems to weaken the copper–acetate bond and result in a higher turnover number.

To support this thesis, DFT calculations were performed to determine the different reaction energies ($[LCu_2(OAc)_2]^+ \rightarrow [LCu_2(OAc)]^{2+} + OAc^-$) for the piperidine, morpholine, and thiomorpholine monocations (**1A–3A**) converting into the corresponding monoacetato-bridged dications in their boat (**1B–3B**) and armchair (**1C–3C**) conformations (Scheme 2). All nine structures and a free acetate anion have been optimized at the B3-LYP/SV(d) level of theory. The resulting relative energies (ΔE), the bond lengths of the coordinating Cu–X linkage of the boat conformers ($R_{Cu\text{-}X}$), and the dihedral angle between the two piperazine nitrogen atoms and the two coordinating oxygen atoms of the left copper center ($\sphericalangle$NNOO), which is a measure for the planarity of the ligand sphere of this metal center, are shown in Table 5.

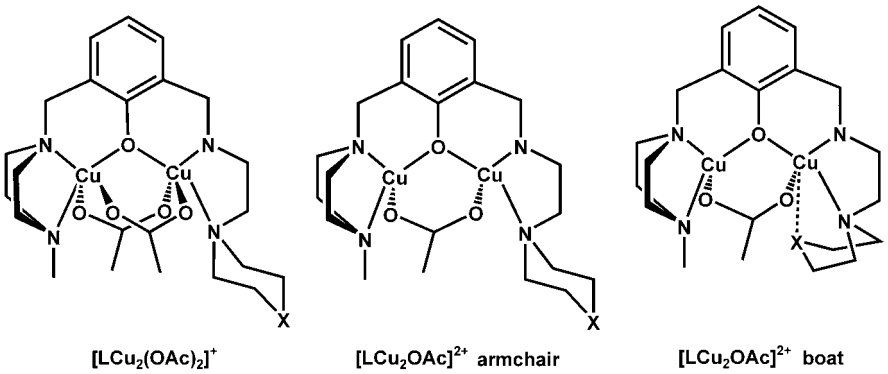

Scheme 2. Structures $[Cu_2(L)(OAc)_2]^+$ and the boat and chair conformations of $[Cu_2(L)(OAc)]^{2+}$ (with X = CH_2 (**1**), O (**2**), and S (**3**)).

For the thiomorpholine system, the isomer with a boat conformation of the subunit (**3B**) is found to be 5.5 kcal mol^{-1} more stable than the corresponding armchair conformer (**3C**). Moreover, the structure of **3B** possesses a linkage of the sulfur atom to one of the copper centers ($R_{Cu\text{-}S} = 2.42$ Å), which clearly indicates that the sulfur atom is capable of displacing the acetate bridge and building a free coordination site for the substrate, thus yielding an almost planar surrounding ($\sphericalangle$NNOO = 2.9°) of the lower-coordinated (left) copper center.

For the morpholine compound, the boat (**2B**) and armchair (**2C**) structures are rather close in energy. **2C** is found

© 2005 Wiley-VCH Verlag GmbH & Co. KGaA, Weinheim

Table 5. Relative energies and structural parameters of the model complexes optimized at the B3-LYP/SV(d) level of theory.

System	X	Ligand conformation	$R_{Cu\text{-}X}$ [Å]	∢NNOO [°]	ΔE [kcal mol^{-1}]
1A: $[LCu_2(OAc)_2]^+$	CH_2				0.0
1B: $[LCu_2(OAc)]^{2+}$ + OAc^-	CH_2	boat	3.12	1.3	196.1
1C: $[LCu_2(OAc)]^{2+}$ + OAc^-	CH_2	armchair		25.4	185.7
2A: $[LCu_2(OAc)_2]^+$	O				0.0
2B: $[LCu_2(OAc)]^{2+}$ + OAc^-	O	boat	2.27	3.0	203.6
2C: $[LCu_2(OAc)]^{2+}$ + OAc^-	O	armchair		25.4	202.2
3A: $[LCu_2(OAc)]^{2+}$	S				0.0
3B: $[LCu_2(OAc)]^{2+}$ + OAc^-	S	boat	2.42	2.9	195.5
3C: $[LCu_2(OAc)]^{2+}$ + OAc^-	S	armchair		25.3	201.0

to be only 1.4 kcal mol^{-1} lower in energy than **2B**. It is also noteworthy in this case that the subunit with the boat conformation is capable of establishing a coordinative bond towards one of the copper centers ($R_{Cu\text{-}O}$ = 2.27 Å), again resulting in an almost planar coordination (∢NNOO = 3.0°) of the other metal center. The methylene group of the piperidine ring in **1** is not able to undergo binding interactions ($R_{Cu\text{-}CH2}$ = 3.12 Å) with the copper ion and, as a result, the chair conformation (**1C**) is significantly stabilized (by 10.4 kcal mol^{-1}) compared to the boat conformation (**1B**) of the piperidine subunit.

By a closer inspection of the molecular structures it can be seen that all isomers carrying a subunit in the boat conformation provide a planar surrounding of the lower-coordinated copper center. The corresponding dihedral angles are found to be 1.3–3.0°, whereas for the corresponding armchair isomer this angle is about 25°. This observation, in combination with the knowledge of the relative stabilities of the isomers in question, provides an explanation for the different reaction rates observed in the kinetic studies. The Cu–X linkage leads for **3**, and to a lesser extent also for **2**, to an unusual stabilization of the boat conformation of the coordinated ligand subunits, whereas for **1** this additional coordinative bond cannot be established. The additional linkage has a more planar uncoordinated metal center as a consequence. This type of coordination geometry clearly enhances the reactivity of this center. With regard to the relative energies, this effect is strongly pronounced with the thiomorpholine ligand (in **3**). For the complex with the morpholine structure (**2**) an equilibrium mixture of both isomers can be expected, whereas in the case with piperidine (**1**) this equilibrium is clearly shifted towards the less-reactive boat conformer, thus providing an explanation for the experimentally observed turnover numbers of the complexes.

To estimate the strength of the Cu–X linkages, knowledge of the relative energies of different conformers of the isolated piperidine (**4**), morpholine (**5**), and thiomorpholine (**6**) subunits are highly desirable (Scheme 3). Although this topic has been previously investigated[68,69] for **4** and **5**, these results were calculated by quantum-chemical methods of different quality and are difficult to compare for the distinct structures. Moreover, it seems necessary to apply the same methods as those used for **1**–**3** to be able to discuss the results in the whole context. For these reasons, we decided to repeat the calculations for the various conformers by using density functional theory and perturbative methods together with larger AO basis sets. For each armchair and boat conformer there exist two possible orientations of the N–H hydrogen atom, either in an equatorial or an axial position. But only two of these conformers, that is, the ones which correspond to the subligand orientation in the model complexes (**1**–**3**), are of relevance for this study: a boat isomer with the N–H in the equatorial position and an armchair isomer with the N–H in the axial position (Scheme 3). The results are shown in Table 6. From the data one can immediately see that the armchair conformations are strongly stabilized compared to the boat conformations for all molecules. The results show only a weak dependency on the applied method and basis set.

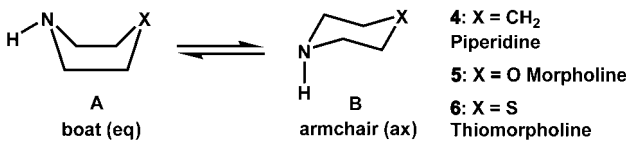

Scheme 3. Piperidine, morpholine, and thiomorpholine conformers.

Table 6. Relative energies of the investigated piperidine, morpholine, and thiomorpholine conformers with respect to their individual armchair (equatorial) conformers [kcal mol^{-1}].

Compound	B3-LYP/ SV(d)	B3-LYP/ TZV(d,p)	MP2[a]/ TZV(d,p)	MP2[a]/ TZV(2df,2pd)
4: piperidine				
A: boat (eq)	7.4	7.3	7.5	7.7
B: armchair (ax)	0.9	0.6	0.8	0.9
5: morpholine				
A: boat (eq)	9.6	9.6	10.2	10.2
B: armchair (ax)	1.1	0.8	1.1	1.0
6: thiomorpholine				
A: boat (eq)	10.0	10.0	10.4	10.2
B: armchair (ax)	0.6	0.5	0.9	0.9

[a] B3-LYP/TZV(d,p)-optimized geometries.

The energy differences are large enough to allow a qualitative discussion, even at the B3-LYP/SV(d) level of theory. For piperidine (**4**) the energetic difference between both isomers is, at 6.5 kcal mol^{-1}, somewhat less than that for the large complexes. This might be due to steric reasons. For morpholine (**5**), the calculation yields an energetic difference of 8.5 kcal mol^{-1}, but in the metal complex this gap is only 1.4 kcal mol^{-1}. This leads to an approximate binding

 © 2005 Wiley-VCH Verlag GmbH & Co. KGaA, Weinheim

energy of the coordinative bond of 7 kcal mol^{-1}. In the case of the thiomorpholine, the energetic order is reversed. For the free ligand (**6**) the energetic difference is 9.4 kcal mol^{-1} in favor of the armchair conformation, whereas for the complex (**3**) the boat conformer is 5.5 kcal mol^{-1} lower in energy than the armchair conformer. The approximated stabilization in the complex amounts to 15 kcal mol^{-1}. This large energetic difference in the gas phase should remain for the complex in solution but probably to a lesser extent. This stabilizing effect and the subsequent influence upon the molecular structure of the model complexes provide a sound explanation for the different reaction rates of the three different compounds.

Furthermore, these results were corroborated by ESI-MS experiments that were performed on methanolic solutions of **1**–**3** (see Figures S7–S9 in the Supporting Information). For all three compounds, evidence for the two cationic species $[Cu_2(L)(OAc)_2]^+$ and $[Cu_2(L)(OAc)]^{2+}$ was found. The relative intensities of the signals underline the results from the DFT calculations and the kinetic investigations. The proportion of complexes with only one acetate bridge rises in the order **1** < **2** < **3** in solution.

Summary

In summary, we have presented the synthesis and characterization of three new compartmental ligands and their dinuclear copper(II) complexes. The utilized ligands were pentadentate μ-phenoxo-bridged and differ in one donor arm that was changed from (*N*-(2-aminoethyl)piperidine to *N*-(2-aminoethyl)-morpholine or *N*-(2-aminoethyl)thiomorpholine. The crystal structures of these three new compounds revealed broad resemblances. Kinetic investigations based on the Michaelis–Menten model showed that the turnover numbers of the complexes increases in the order **1** < **2** < **3**. DFT calculations and ESI-MS experiments support the thesis that a higher affinity of the group in the position 4 of the piperidine ring of the ligand to the copper ion enhances removal of one acetate bridge. The resulting free coordination site can be used for substrate binding, thereby resulting in higher turnover numbers for the catechol oxidation. The presented compounds are excellent models for the active site of catechol oxidase that mimic the short copper–copper distance of approximately 3 Å as well as the dissimilar environment of the metal ions, including a thioether bond in **3**. The electronic spectra of all three compounds show typical features of copper(II) complexes.

Acknowledgements

Financial support from the Deutsche Forschungsgemeinschaft (Program SFB 424—Molecular Orientation and its Functions in Chemical Systems) and the Fonds der Chemischen Industrie is gratefully acknowledged.

[1] E. I. Solomon, U. M. Sundaram, T. E. Machonkin, *Chem. Rev.* **1996**, *96*, 2563.
[2] J. Bonaventura, C. Bonaventura, *Am. Zool.* **1980**, *20*, 7.
[3] T. T. Herskovitz, *Comp. Biochem. Physiol.* **1988**, *91*, 597.
[4] H. S. Mason, *Nature* **1956**, *177*, 79.
[5] F. Kubowitz, *Biochem. Z.* **1937**, *292*, 222.
[6] F. Kubowitz, *Biochem. Z.* **1938**, *299*, 32.
[7] A. M. Mayer, E. Harel, *Phytochemistry* **1979**, *18*, 193.
[8] Y. M. Jiang, J. R. Fu, G. Zauberman, Y. Fuchs, *J. Sci. Food Agric.* **1999**, *79*, 950.
[9] B. Paul, L. R. Gowda, *J. Agric. Food Chem.* **2000**, *48*, 3839.
[10] C. P. Yang, S. Fujita, S. M. Ashrafuzzaman, N. Nakamura, N. Hayashi, *J. Agric. Food Chem.* **2000**, *48*, 2732.
[11] F. Bilka, A. Balazova, A. Bilkova, M. Psenak, *Pharmazie* **2000**, *55*, 155.
[12] P. Mazzafera, S. P. Robinson, *Phytochemistry* **2000**, *55*, 285.
[13] A. Rompel, H. Fischer, D. Meiwes, K. Büldt-Karentzopoulos, R. Dillinger, F. Tuczek, H. Witzel, B. Krebs, *J. Biol. Inorg. Chem.* **1999**, *4*, 56.
[14] T. Klabunde, C. Eicken, J. C. Sacchettini, B. Krebs, *Nat. Struct. Biol.* **1998**, *5*, 1084.
[15] K. Lerch, *J. Biol. Chem.* **1982**, *257*, 6414.
[16] C. Gielens, N. De Geest, X. Q. Xin, B. Devreese, J. Ban Beeumen, G. Preaux, *Eur. J. Biochem.* **1997**, *248*, 879.
[17] M. E. Muff, K. I. Miller, K. E. van Holde, W. A. Hendrickson, *J. Mol. Biol.* **1998**, *278*, 855.
[18] N. Ito, S. E. V. Phillips, K. D. S. Yadav, P. F. Knowles, *J. Mol. Biol.* **1994**, *238*, 794.
[19] T. Kruse, T. Weyhermüller, K. Wieghardt, *Inorg. Chim. Acta* **2002**, *331*, 81.
[20] L. M. Mirica, X. Ottenwaelder, T. D. P. Stack, *Chem. Rev.* **2004**, *104*, 1013.
[21] E. A. Lewis, W. B. Tolman, *Chem. Rev.* **2004**, *104*, 1047.
[22] K. D. Karlin, S. Kaderli, A. D. Zuberbühler, *Acc. Chem. Res.* **1997**, *30*, 139.
[23] S. Fox, K. D. Karlin, *Active Oxygen in Biochemistry* (Eds.: J. S. Valentine, C. S. Foote, A. Greenberg, J. F. Liebman), Chapman & Hall, Glasgow, **1995**, p. 188.
[24] N. Kitajima, W. B. Tolman, *Prog. Inorg. Chem.* **1995**, *43*, 419.
[25] W. B. Tolman, *Acc. Chem. Res.* **1997**, *30*, 227.
[26] E. I. Solomon, F. Tuczek, D. E. Root, C. A. Brown, *Chem. Rev.* **1994**, *94*, 827.
[27] N. Kitajima, Y. Moro-oka, *Chem. Rev.* **1994**, *94*, 737.
[28] K. D. Karlin, Z. Tyeklár, *Adv. Inorg. Biochem.* **1994**, *9*, 123.
[29] N. Kitajima, Y. Moro-oka, *J. Chem. Soc. Dalton Trans.* **1993**, 2665.
[30] T. N. Sorrell, *Tetrahedron* **1989**, *45*, 3.
[31] Z. Tyeklár, K. D. Karlin, *Acc. Chem. Res.* **1989**, *22*, 241.
[32] K. D. Karlin, Y. Gultneh, *Prog. Inorg. Chem.* **1987**, *35*, 219.
[33] C. Belle, J.-L. Pierre, *Eur. J. Inorg. Chem.* **2003**, 4137.
[34] S. Torelli, C. Belle, S. Hamman, J.-L. Pierre, *Inorg. Chem.* **2002**, *41*, 3983.
[35] C. Eicken, B. Krebs, J. C. Sacchettini, *Curr. Opin. Struct. Biol.* **1999**, *9*, 677.
[36] K. D. Karlin, Y. Gultneh, T. Nicholson, J. Zubieta, *Inorg. Chem.* **1985**, *24*, 3727.
[37] J. Ackermann, F. Meyer, E. Kaifer, H. Pritzkow, *Chem. Eur. J.* **2002**, *8*, 247.
[38] I. A. Koval, M. Huisman, A. F. Stassen, P. Gamez, M. Lutz, A. L. Spek, J. Reedijk, *Eur. J. Inorg. Chem.* **2004**, 591.
[39] I. A. Koval, D. Pursche, A. F. Stassen, P. Gamez, B. Krebs, J. Reedijk, *Eur. J. Inorg. Chem.* **2003**, 1669.
[40] N. Möller, M. Lüken, B. Krebs, *J. Inorg. Biochem.* **2001**, *86*, 344.
[41] M. S. Nasir, K. D. Karlin, D. McGowty, J. Zubieta, *J. Am. Chem. Soc.* **1991**, *113*, 698.
[42] J. Reim, B. Krebs, *J. Chem. Soc. Dalton Trans.* **1997**, 3893.
[43] N. N. Murthy, M. Mahroof-Tahir, K. D. Karlin, *Inorg. Chem.* **2001**, *40*, 628.

© 2005 Wiley-VCH Verlag GmbH & Co. KGaA, Weinheim

[44] C. Fernandes, A. Neves, A. J. Bortoluzzi, A. S. Mangrich, E. Rentschler, B. Szpoganicz, E. Schwingel, *Inorg. Chim. Acta* **2001**, *320*, 12.
[45] C. Eicken, F. Zippel, K. Büldt-Karentzopoulos, B. Krebs, *FEBS Lett.* **1998**, *436*, 293.
[46] H. Adams, G. Candeland, J. D. Crane, D. E. Fenton, A. J. Smith, *J. Chem. Soc. Chem. Commun.* **1990**, 93.
[47] J. D. Crane, D. E. Fenton, J.-M. Latour, A. J. Smith, *J. Chem. Soc. Dalton Trans.* **1991**, 2979.
[48] L. D. Wise, G. C. Morrison, K. Egan, M. A. Commarato, G. Kopia, E. C. Lattime, *J. Med. Chem.* **1974**, *17*, 1232.
[49] G. M. Sheldrick, SHELX-97, Universität Göttingen, **1997**.
[50] CCDC-244275, CCDC-244276, and CCDC-244277 contain the supplementary crystallographic data for this paper. These data can be obtained free of charge via www.ccdc.cam.ac.uk/conts/retrieving.html (or from the Cambridge Crystallographic Data Centre, 12 Union Road, Cambridge CB2 1EZ, UK; fax: (+44) 1223–336–033; or deposit@ccdc.cam.uk).
[51] R. Ahlrichs, M. Bär, H.-P. Baron, R. Bauernschmitt, S. Böcker, M. Ehring, K. Eichkorn, S. Elliott, F. Furche, F. Haase, M. Häser, H. Horn, C. Huber, U. Huniar, M. Kattannek, C. Kölmel, M. Kollwitz, K. May, C. Ochsenfeld, H. Öhm, A. Schäfer, U. Schneider, O. Treutler, M. von Arnim, F. Weigend, P. Weis, H. Weiss, TURBOMOLE (Version 5.3), Universität Karlsruhe, **2000**.
[52] A. D. Becke, *J. Chem. Phys.* **1993**, *98*, 5648.
[53] C. Lee, W. Yang, R. G. Parr, *Phys. Rev. B* **1988**, *37*, 785.
[54] F. Weigend, M. Häser, *Theor. Chem. Acc.* **1997**, *97*, 331.
[55] The basis sets are available from the TURBOMOLE homepage (http://www.turbomole.com) through the FTP Server button (in the subdirectories basen, jbasen, and cbasen).
[56] A. Schäfer, H. Horn, R. Ahlrichs, *J. Chem. Phys.* **1992**, *97*, 2571.
[57] A. Schäfer, C. Huber, R. Ahlrichs, *J. Chem. Phys.* **1994**, *100*, 5829.
[58] A. W. Addison, A. N. Rao, J. Reedjik, J. Rijn, G. C. Verschoor, *J. Chem. Soc. Dalton Trans.* **1984**, 1349; definition of τ: τ=(largest bond angle − second largest bond angle)/60, that is $\tau=1$ for trigonal bipyramidal, $\tau=0$ for square pyramidal.
[59] E. I. Solomon, K. W. Penfield, D. E. Wilcox, *Struct. Bonding (Berlin)* **1983**, *53*, 1.
[60] P. K. Coughlin, S. J. Lippard, *J. Am. Chem. Soc.* **1981**, *103*, 3228.
[61] K. D. Karlin, A. Farooq, J. C. Hayes, B. I. Cohen, T. M. Rowe, E. Sinn, J. Zubieta, *Inorg. Chem.* **1987**, *26*, 1271.
[62] Y. Nakao, Y. Oohata, Y. Fujiwara, M. Itadani, T. Sakurai, A. Ichimura, W. Mori, *Bull. Chem. Soc. Jpn.* **1993**, *66*, 2112.
[63] K. D. Karlin, I. Sanyal, A. Farooq, R. R. Jacobson, S. N. Shaikh, J. Zubieta, *Inorg. Chim. Acta* **1990**, *174*, 13.
[64] E. W. Ainscough, A. G. Bingham, A. M. Brodie, J. M. Husbands, J. E. Plowman, *J. Chem. Soc. Dalton Trans.* **1981**, 1701.
[65] K. Bertoncello, G. D. Fallon, J. H. Hodgkin, K. S. Murray, *Inorg. Chem.* **1988**, *27*, 4750.
[66] B. J. Hathaway, *J. Chem. Soc. Dalton Trans.* **1972**, 1196.
[67] B. J. Hathaway in *Comprehensive Coordination Chemistry, Vol. 5* (Ed.: G. Wilkinson), Pergamon, New York, **1987**, 553.
[68] A. L. Capparelli, J. Marañon, O. M. Sobarrain, R. R. Filgueira, *J. Mol. Struct.* **1974**, *23*, 145.
[69] M. Ladika, N. G. Rondan, *J. Mol. Struct.* **1996**, *365*, 21.

Received: July 27, 2004
Published online: December 27, 2004

 © 2005 Wiley-VCH Verlag GmbH & Co. KGaA, Weinheim